

## Infrared spectra of proton irradiated ices containing methanol

M. H. Moore,<sup>1</sup> R. F. Ferrante<sup>2</sup> and J. A. Nuth III<sup>1</sup>

<sup>1</sup>NASA/Goddard Space Flight Center, Astrochemistry Branch, Greenbelt, MD 20771, U.S.A.

<sup>2</sup>U.S. Naval Academy, Department of Chemistry, Annapolis, MD 21402, U.S.A.

Received 13 June 1995; revised 11 September 1995; accepted 11 September 1995

**Abstract.** A set of experimental results on the spectral identification of new species synthesized in irradiated CH<sub>3</sub>OH and H<sub>2</sub>O + CH<sub>3</sub>OH ices is reported. Mass spectroscopy of volatile species released during slow warming gives supporting information on identifications. H<sub>2</sub>CO is the dominant volatile species identified in the irradiated ices. CH<sub>4</sub>, CO and CO<sub>2</sub> are also formed. During warming the ice evolves into a residual film near 200 K, whose features are similar to those of ethylene glycol along with a C=O bonded molecular group. Irradiation simulates expected cosmic ray processing of ices in comets stored in the Oort cloud region for 4.6 billion years. Results support the idea that a comet originally containing an H<sub>2</sub>O + CH<sub>3</sub>OH ice component has a decreasing concentration of CH<sub>3</sub>OH towards its outer, most heavily irradiated layers (if independent of all other sources and sinks). The CH<sub>4</sub>/CO and CO/CO<sub>2</sub> ratios are calculated as a function of irradiation: after 22 eV per molecule, CH<sub>4</sub>/CO = 1.96 and CO/CO<sub>2</sub> = 1.45 in an H<sub>2</sub>O + CH<sub>3</sub>OH ice mixture. Infrared spectra of CH<sub>3</sub>OH at *T* < 20 K on amorphous silicate smokes show a predominantly crystalline phase ice. Irradiation of the ice/silicate composite is compared with irradiated CH<sub>3</sub>OH on aluminum substrates. Implication for cometary type ices are discussed. Published by Elsevier Science Ltd

### Introduction

Water ice and H<sub>2</sub>O-dominated icy mixtures are important constituents of cometary nuclei (Spinrad, 1987; Mumma *et al.*, 1986; Combes *et al.*, 1988) and interstellar grains (Tielens, 1989). Icy mixtures include molecules more volatile than H<sub>2</sub>O such as CH<sub>3</sub>OH, H<sub>2</sub>CO, NH<sub>3</sub>, CO<sub>2</sub>, CO and CH<sub>4</sub> (e.g. Mumma *et al.* (1993a) and references therein). Relative to H<sub>2</sub>O, the abundance of CH<sub>3</sub>OH is a few per-

cent in many comets, and CH<sub>3</sub>OH is likely to be a major component in interstellar ice (Allamandola *et al.*, 1988). The CH<sub>3</sub>OH abundance relative to H<sub>2</sub>O in the solid phase is near 7% based on interstellar observations of the CH stretching mode near 3.5  $\mu$ m (e.g. Grim *et al.*, 1991). However, there is some variation from cloud to cloud and some controversy about the ratio. More recent results from Skinner *et al.* (1992) provide data on the 9.7  $\mu$ m feature attributed to CH<sub>3</sub>OH. This report focuses on laboratory studies of ion irradiated CH<sub>3</sub>OH and H<sub>2</sub>O + CH<sub>3</sub>OH ices. The infrared (IR) spectra of these ice films are used to identify the synthesized products, and to record any differences when these ices are irradiated as ice/silicate composites. In these experiments irradiation simulates expected cosmic ray processing of ices, and smokes are used as laboratory analogs for interstellar-type silicate grains.

Several factors can affect the spectra of ices including formation and storage conditions, the exposure to a radiation environment and the incorporation of dust. The amorphous and crystalline phases of ices, whose formation and stability depend on temperature and growth rate (Kouchi *et al.*, 1994) have different spectral features. Various thermal histories of an ice can cause both reversible and irreversible changes in the IR spectrum. These effects have been discussed in some details for H<sub>2</sub>O ice by Hobbs (1974), Hagen *et al.* (1983) and Moore and Hudson (1992, 1994). The amorphization of crystalline H<sub>2</sub>O ice induced by ion irradiation (Baratta *et al.*, 1991; Strazzulla *et al.*, 1991; Moore and Hudson, 1992) is demonstrated by IR spectral changes; similar amorphization has been demonstrated for CH<sub>3</sub>OH ice (Hudson and Moore, 1995). Exposure to photon and ion radiation processing also results in the synthesis of new species, which adds new features to the original spectrum (Allamandola *et al.*, 1988; Moore *et al.*, 1983; Strazzulla *et al.*, 1991). Another factor which can influence the shape of spectral features is the inclusion of grains. The presence of small grains in an ice mixture has been used to model not only the 3.1  $\mu$ m band shape of H<sub>2</sub>O ices, matching the spectra observed in interstellar molecular clouds (e.g. Greenberg,

1991), but the 45  $\mu\text{m}$  emission band of  $\text{H}_2\text{O}$  seen in circumstellar nebulae (Omont *et al.*, 1990). Recently, Moore *et al.* (1994) reported that both  $\text{H}_2\text{O}$  and  $\text{CH}_3\text{OH}$  formed crystalline phase ices, rather than the amorphous phase expected, when deposited onto silicate smoke layers at  $T < 20$  K.

In the laboratory, gas, liquid and solid phase irradiations of  $\text{CH}_3\text{OH}$  result in the formation of  $\text{H}_2$ , glycol, and  $\text{H}_2\text{CO}$ , sometimes with smaller amounts of  $\text{CH}_4$  and  $\text{CO}$  (Porter and Noyes (1959), UV photolysis of  $\text{CH}_3\text{OH}$  gas; Baxendale and Mellows (1961),  $\gamma$ -irradiated  $\text{CH}_3\text{OH}$  liquid; Kalyazin and Kovalev (1978),  $\gamma$ -irradiated  $\text{CH}_3\text{OH}$  solid). Yields of  $\text{H}_2$ , ethylene glycol ( $(\text{CH}_2\text{OH})_2$ ), and  $\text{H}_2\text{CO}$  for solid  $\text{CH}_3\text{OH}$  irradiated at 77 K are approximately 3.5, 3, and 1 molecules/100 eV, respectively (Kalyazin and Kovalev, 1978). These yields were determined by chemical analysis of both the gas and liquid after warming the irradiated ice. The IR spectrum of  $\text{H}_2\text{O} + \text{CH}_3\text{OH}$  ice after UV photolysis shows the formation of  $\text{H}_2\text{CO}$ ,  $\text{CO}$ ,  $\text{CO}_2$ , and  $\text{CH}_4$  at  $T < 20$  K (Allamandola *et al.*, 1988); they conclude that the principal product is  $\text{H}_2\text{CO}$ . Previous studies by Moore and Khanna (1991) reported the identification of  $\text{H}_2\text{CO}$ ,  $\text{CO}$ ,  $\text{CO}_2$ ,  $\text{CH}_4$ , and ethanol ( $\text{C}_2\text{H}_5\text{OH}$ ) in proton irradiated pure  $\text{CH}_3\text{OH}$  and  $\text{CH}_3\text{OH} + \text{H}_2\text{O}$  ices. Baratta *et al.* (1994) identified the formation of  $\text{CO}$ ,  $\text{CO}_2$ ,  $\text{CH}_4$ , and  $\text{H}_2\text{O}$  in the IR spectrum of 3 keV  $\text{He}^+$  bombarded  $\text{CH}_3\text{OH}$  and  $\text{H}_2\text{O} + \text{CH}_3\text{OH}$  ices. They concluded that the largest yield was for a  $\text{C}=\text{O}$  bonded feature which could only partially be explained by the synthesis of  $\text{H}_2\text{CO}$ . The possible contribution of acetone ( $(\text{CH}_3)_2\text{CO}$ ) was also discussed.

We report in this paper a set of experimental results on the spectral identification of new species synthesized in irradiated  $\text{CH}_3\text{OH}$  and  $\text{H}_2\text{O} + \text{CH}_3\text{OH}$  at  $T < 20$  K. Ratios of  $\text{CH}_4/\text{CO}$  and  $\text{CO}/\text{CO}_2$  are calculated as a function of eV molecule $^{-1}$  and compared with data for similar ices irradiated with  $\text{He}^+$  to higher doses. Mass spectra of gases released during warming result in supporting information about new products. Spectra of ices warmed to temperatures near 200 K are fitted with the spectrum of a possible less volatile residual product. Implications for cometary type ices are discussed.

## Experimental procedures

Ices are grown on an aluminum mirror substrate cooled to  $T < 20$  K in a closed-cycle cryostat. Surrounding the substrate is a six-sided chamber designed for a variety of *in situ* measurements. The chamber pressure is reduced to below  $6 \times 10^{-10}$  bar using an ion pump. The ice film can be rotated to face in different directions depending on the type of measurement: IR spectroscopy, mass spectroscopy, or proton irradiation.

IR absorption spectra of thin ice films are recorded with a Mattson (Polaris) FTIR. The technique used results in a transmission–reflection–transmission spectrum. Typically a spectrum is 60 scan accumulations, with a resolution of 4  $\text{cm}^{-1}$ . Single-beam spectra are ratioed with a background spectrum recorded before any ice deposition. Ices are formed from triply distilled  $\text{H}_2\text{O}$  with a resistance greater

than  $10^7$  ohm cm;  $\text{CH}_3\text{OH}$  was Fisher HPLC grade (99.9% pure). Both liquids had dissolved gases removed by freeze–pump–thaw cycling. Mixtures were made in glass bulbs and the relative composition of the ice was determined using the IR spectrum. An  $\text{H}_2\text{O}/\text{CH}_3\text{OH}$  abundance ratio near 2 was chosen so that our results would be comparable with other published data. Although this ratio is rich in  $\text{CH}_3\text{OH}$  compared to cosmic ices, dilution reduces the IR intensity of the products we want to identify. Thin films of ice, about 4  $\mu\text{m}$  in depth, were grown at 10  $\mu\text{m h}^{-1}$ . Film thickness was monitored by a laser interferometric method. A Dycor quadrupole mass spectrometer is used to detect volatile species released from the ice during warming. The radiation source was a 1 MeV proton beam from a Van de Graaff accelerator. This energy proton penetrates 22  $\mu\text{m}$  of  $\text{H}_2\text{O}$  ice. The experiment is designed so that the integrated beam current measured in the aluminum substrate is a direct measure of the incident fluence ( $\text{p}^+ \text{cm}^{-2}$ ). Details of this experimental set-up are given in Moore and Hudson (1992).

Silicate smokes are made in a separate grain condensation chamber by either evaporation of  $\text{SiO}$  solid or by combustion of  $\text{SiH}_4$  with  $\text{O}_2$  followed by vapor phase nucleation and growth in an  $\text{H}_2$  atmosphere. The smokes are deposited onto the aluminum mirror substrates and then these coated substrates are attached to the tail section of the cryostat and cooled to  $T < 20$  K prior to the condensation of  $\text{CH}_3\text{OH}$  or  $\text{H}_2\text{O} + \text{CH}_3\text{OH}$  gases. A discussion of the physical nature of these smokes, their 10  $\mu\text{m}$  spectra, and spectra of a variety of gases deposited on these smokes is given in Moore *et al.* (1994) and references therein.

## Experiments and results

The IR spectrum of pure  $\text{CH}_3\text{OH}$  deposited on an aluminum mirror substrate at  $T < 20$  K is compared in Fig. 1 with the spectrum of that ice after irradiation to a total dose of 34 eV molecule $^{-1}$ . New features in the irradiated ice are marked with an asterisk. The identification of these features and their positions are summarized in Table 1. New products easiest to identify are: the  $\text{C}=\text{O}$  stretch and  $\text{C}=\text{O}$  bend of  $\text{CO}_2$ ,  $\text{CO}$ , the  $\text{HCO}$  radical, and the  $\text{C}-\text{H}$  deformation of  $\text{CH}_4$ . The feature at 1721  $\text{cm}^{-1}$  is due in part to the  $\text{C}=\text{O}$  stretch of  $\text{H}_2\text{CO}$ . The small shoulder at 1497  $\text{cm}^{-1}$  fits with the  $\text{CH}_2$  scissors mode of  $\text{H}_2\text{CO}$  and the 1246  $\text{cm}^{-1}$  feature with the  $\text{CH}_2$  in-plane bend of  $\text{H}_2\text{CO}$ . The 1091  $\text{cm}^{-1}$  feature is identified as the  $\text{C}-\text{O}$  stretch mode of  $\text{C}_2\text{H}_5\text{OH}$ . The relative strengths of these features vary with dose. Although, pure amorphous phase  $\text{CH}_3\text{OH}$  ice converts to a crystalline phase during warming to  $T \sim 130$  K, similar phase changes are not observed for the irradiated  $\text{CH}_3\text{OH}$  ice shown in Fig. 1.

Figure 2 shows the IR spectrum of  $\text{H}_2\text{O} + \text{CH}_3\text{OH}$  (1:0.6) before and after irradiation to a total dose of 22 eV molecule $^{-1}$ . All synthesized features are marked with an asterisk and their positions are included in Table 1.  $\text{CO}_2$ ,  $\text{CO}$ ,  $\text{CH}_4$ , and the  $\text{HCO}$  radical are identified. The 1850–600  $\text{cm}^{-1}$  spectral region is expanded in Fig. 3a and

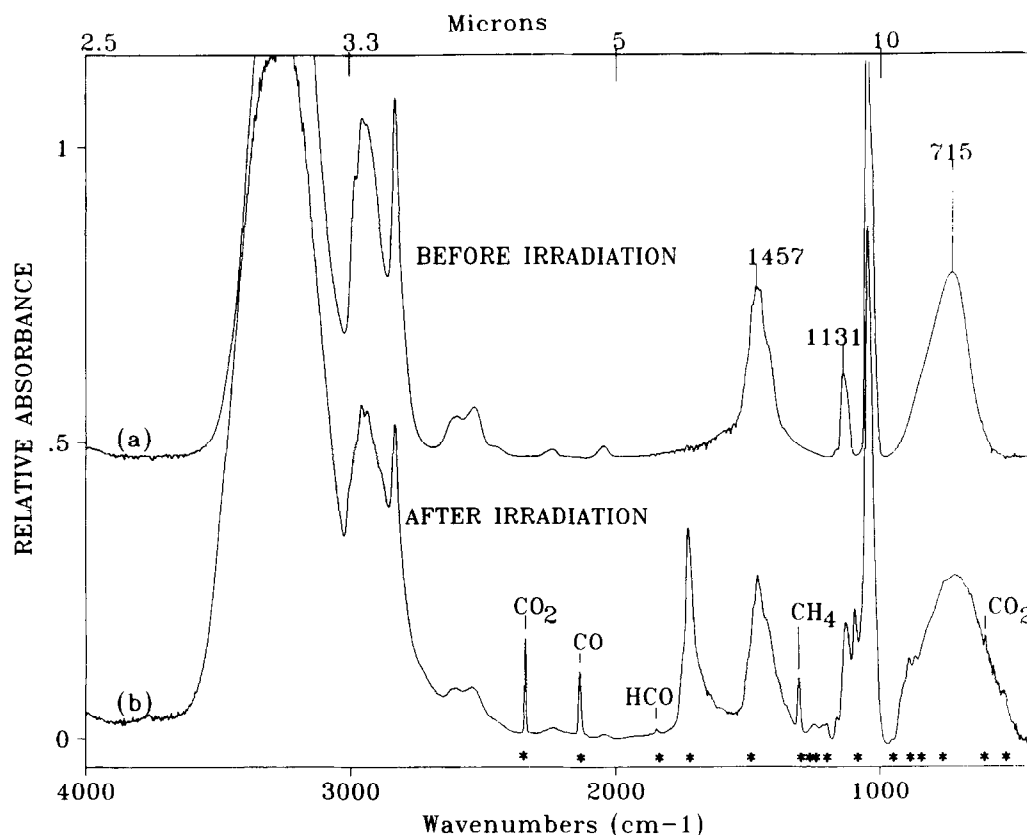


**Fig. 1.** (a) Infrared spectrum of a pure  $\text{CH}_3\text{OH}$  ice film deposited at  $T < 20$  K. (b) Spectrum of the same ice after proton irradiation at  $T < 20$  K to a dose of  $34 \text{ eV molecule}^{-1}$ . Many synthesized features are marked with asterisks; identifications and positions are listed in Table 1

**Table 1.** Identification and position of infrared features for synthesized products in  $\text{CH}_3\text{OH}$  and  $\text{H}_2\text{O} + \text{CH}_3\text{OH}$  ices

Identification	Proton irr. $\text{CH}_3\text{OH}^a$ Position ( $\text{cm}^{-1}$ )	Proton irr. $\text{H}_2\text{O} + \text{CH}_3\text{OH}^a$ Position ( $\text{cm}^{-1}$ )	Proton irr. $\text{H}_2\text{O} + \text{CH}_3\text{OH}^b$ Position ( $\text{cm}^{-1}$ )	UV photolysis <sup>c</sup> $\text{H}_2\text{O} + \text{CH}_3\text{OH}$ Position ( $\text{cm}^{-1}$ )	Vibrational mode
$\nu_3 \text{CH}_4$		3011		3012	C—H st
$\nu_3 \text{CO}_2$	2339	2341	2340	2343	C=O st
$\nu_3 \text{}^{13}\text{CO}_2$		2276			C=O st
CO	2134	2135		2137	C=O st
HCO	1844	1845		1850	
$\nu_2 \text{H}_2\text{CO}$	1721	1713	1722 1743	1720	C=O st
$\nu_3 \text{H}_2\text{CO}$	1497 sh	1499 1355		1500	$\text{CH}_2$ scissor
$\nu_4 \text{CH}_4$	1302	1305	1302	1304	C—H def.
$\nu_6 \text{H}_2\text{CO}$	1246	1250			$\text{CH}_2$ bend
$\text{C}_2\text{H}_5\text{OH}$	1211, 1198 1091	1219, 1185, 1161 w 1089	1263, 1213, 1196 1090		
$\text{CO}_2$	952, 919, 887, 864, 748 650	657	887, 865	657	C=O bend
$(\text{CH}_3)_2\text{CO}^d$	532–516		523		hindered rotation

<sup>a</sup>Ice formed on an aluminum substrate (Figs 1–3).

<sup>b</sup>Ice formed on a silicate smoke (Fig. 6).

<sup>c</sup>Allamandola *et al.* (1988).

<sup>d</sup>Tentative.

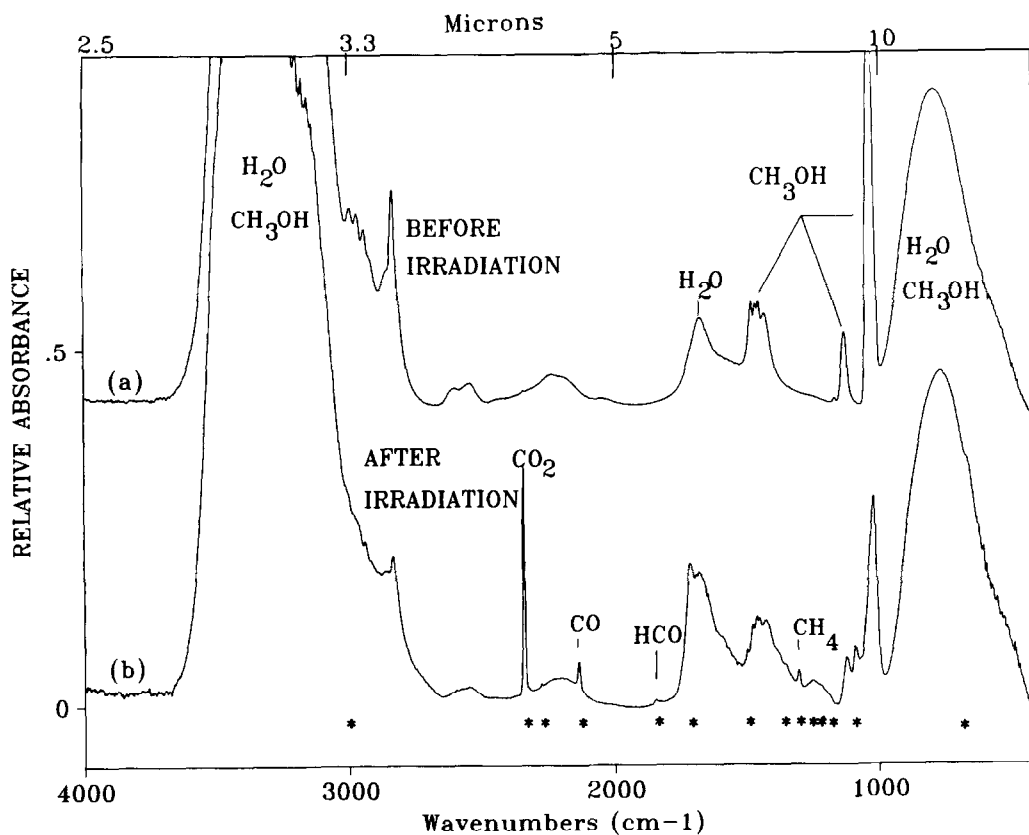


Fig. 2. (a) Infrared spectrum of an  $\text{H}_2\text{O}+\text{CH}_3\text{OH}$  ( $\sim 1:0.6$ ) ice film deposited at  $T < 20$  K. (b) The same ice after proton irradiation at 20 K to a dose of  $22 \text{ eV molecule}^{-1}$ . Many synthesized features are marked with asterisks; identifications and positions are listed in Table 1

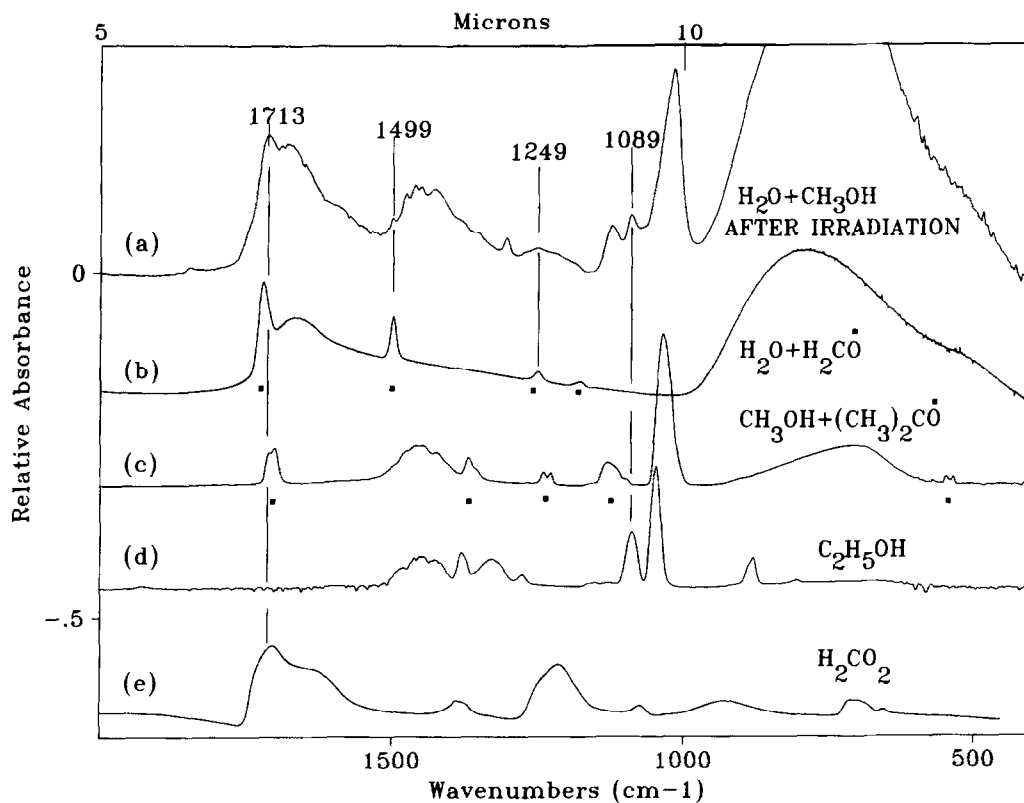
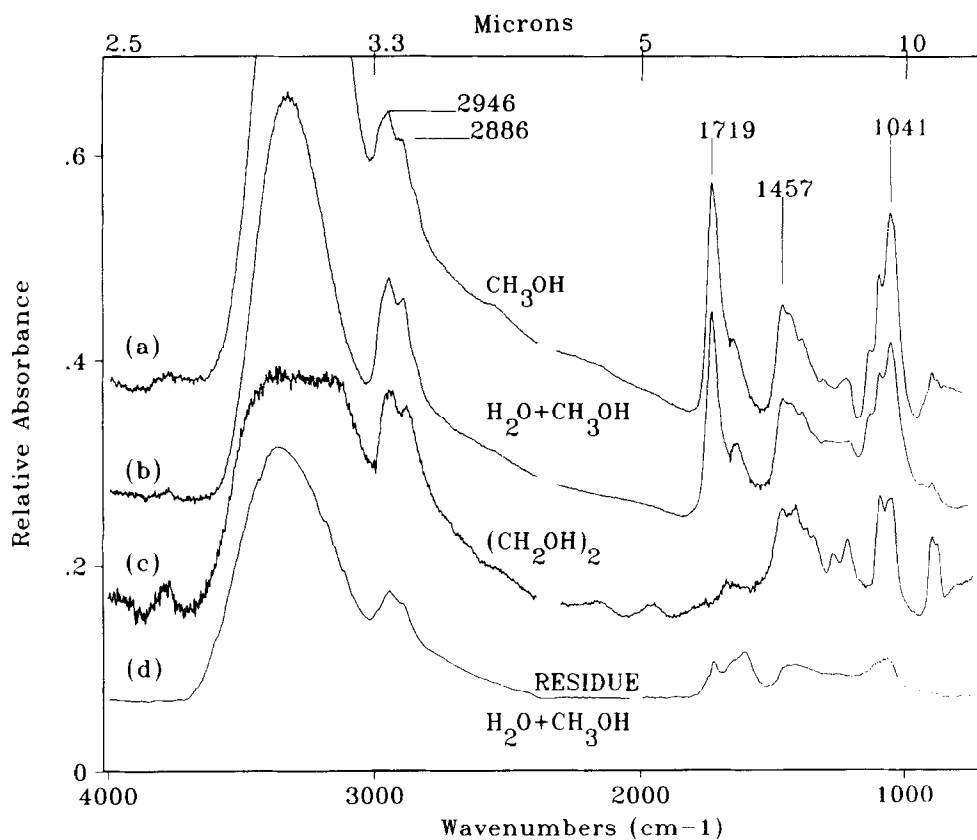


Fig. 3. The  $2000\text{--}400 \text{ cm}^{-1}$  spectral region of irradiated  $\text{H}_2\text{O}+\text{CH}_3\text{OH}$  (Fig. 2a) is compared with spectra of icy mixtures (b)  $\text{H}_2\text{O}+\text{H}_2\text{CO}$  and (c)  $\text{CH}_3\text{OH}+(\text{CH}_3)_2\text{CO}$ . Pure ice spectra are: (d)  $\text{C}_2\text{H}_5\text{OH}$  and (e)  $\text{H}_2\text{CO}_2$ . All spectra were measured at  $T < 20$  K. Peaks marked with a "■" are identified with the component of the mixture similarly marked. Several vertical lines have been drawn to help locate the position of peaks



**Fig. 4.** The infrared spectra of residual films from irradiated (a)  $\text{CH}_3\text{OH}$  and (b)  $\text{H}_2\text{O}+\text{CH}_3\text{OH}$  ices after warming to near 200 K are compared with the spectrum of ethylene glycol,  $(\text{CH}_2\text{OH})_2$ , at 170 K. Spectrum (d) shows the room temperature RESIDUE of similarly irradiated  $\text{H}_2\text{O}+\text{CH}_3\text{OH}$  ice (irradiated at 20 K)

compared with several reference spectra: (b)  $\text{H}_2\text{O}+\text{H}_2\text{CO}$ , (c)  $\text{CH}_3\text{OH}+\text{acetone } ((\text{CH}_3)_2\text{CO})$ , (d)  $\text{C}_2\text{H}_5\text{OH}$ , and (e) formic acid ( $\text{H}_3\text{CO}_2$ ). The  $1713\text{ cm}^{-1}$  feature in the irradiated ice is partially attributed to the  $\text{C}=\text{O}$  stretch of  $\text{H}_2\text{CO}$  (shifted by  $7\text{ cm}^{-1}$ ) combined with the  $\text{O}-\text{H}$  bend mode of  $\text{H}_2\text{O}$ . The  $1499$  and  $1249\text{ cm}^{-1}$  features in spectrum (a) are fitted with  $\text{H}_2\text{CO}$  also. Spectrum (d) of ethanol at  $T < 20\text{ K}$  is a good match with the  $1089\text{ cm}^{-1}$  feature in the irradiated ice. The strongest ethanol feature in spectrum (d) contributes to the broadening of the  $1014\text{ cm}^{-1}$   $\text{CH}_3\text{OH}$  peak in the irradiated ice. It has been suggested by Baratta *et al.* (1994) that acetone could contribute to the  $1713\text{ cm}^{-1}$  feature (compare spectrum (c) with spectrum (a)). One argument in favor of some  $(\text{CH}_3)_2\text{CO}$  is that it was the only simple molecule we examined that has a feature in the  $530\text{ cm}^{-1}$  region which is similar to a weak feature measured in both pure irradiated  $\text{CH}_3\text{OH}$  and  $\text{H}_2\text{O}+\text{CH}_3\text{OH}$ . In this report, the best signal to noise ratio measured for this feature is in irradiated  $\text{CH}_3\text{OH}$  ice shown in Fig. 1b (an asterisk is near  $530\text{ cm}^{-1}$ ).

Standard curve fitting techniques were used to separate the  $1713\text{ cm}^{-1}$  and the  $(\text{OH})\ 1657\text{ cm}^{-1}$  components in Fig. 3a. The integrated absorbance of the  $1713\text{ cm}^{-1}$  feature and the  $1499\text{ cm}^{-1}$  feature were obtained. By comparing the relative integrated areas of these features with those in  $\text{H}_2\text{O}+\text{H}_2\text{CO}$ , we estimated that only  $\sim 25\%$  of the  $1713\text{ cm}^{-1}$  area in  $\text{H}_2\text{O}+\text{CH}_3\text{OH}$  was due to  $\text{H}_2\text{CO}$ . Mass spectra of gases vaporized from irradiated  $\text{CH}_3\text{OH}$

during warming near 160 K showed mass 29 and 30 peaks, and a mass 60 peak; these are consistent with  $\text{HCO}$ ,  $\text{H}_2\text{CO}$ , and  $(\text{H}_2\text{CO})_2$ . Also observed in this temperature range was a mass 58 peak coupled with a mass 43 peak and this observation fits a pattern for  $(\text{CH}_3)_2\text{CO}$  and its fragment  $\text{CH}_3\text{CO}$  (based on mass spectra of slowly vaporized  $(\text{CH}_3)_2\text{CO}$  ices in our laboratory). Similar results were observed for irradiated  $\text{H}_2\text{O}+\text{CH}_3\text{OH}$ , although detection of any masses at 58 and 43 did not occur until the temperature was near 180–190 K. These mass signals add support for the presence of some acetone, however more confidence in this assignment will require experiments with isotopically labelled components. Both  $\text{CH}_3\text{OH}$  and  $\text{H}_2\text{O}+\text{CH}_3\text{OH}$  irradiated ices evolve with warming into a residual film near 200 K. These less volatile materials are of interest since similar synthesized molecules of low volatility may be present in cometary and precometary ices.

The  $1721$  and  $1713\text{ cm}^{-1}$  absorption peaks in irradiated  $\text{CH}_3\text{OH}$  and  $\text{H}_2\text{O}+\text{CH}_3\text{OH}$  ices (respectively) are part of a broad feature which remains stable on warming to room temperature, suggesting that there are contributions to this  $\text{C}=\text{O}$  stretch (st) region from molecules which are less volatile than  $\text{H}_2\text{CO}$  and  $(\text{CH}_3)_2\text{CO}$ . Slow warming of  $\text{H}_2\text{O}+\text{H}_2\text{CO}$  ices shows release of  $\text{H}_2\text{CO}$  before 150 K;  $(\text{CH}_3)_2\text{CO}$  ice vaporizes near 150 K. Figure 4 compares the IR spectra of several residual films; trace (a) is the residual spectrum of irradiated  $\text{CH}_3\text{OH}$  ice warmed to 220 K, spectrum (b) shows the residual signature of irradiated

H<sub>2</sub>O+CH<sub>3</sub>OH warmed to 190 K. These two spectra are nearly indistinguishable. Spectrum (c) is ethylene glycol ((CH<sub>2</sub>OH)<sub>2</sub>) at  $T = 170$  K. Ethylene glycol has similar 3.4  $\mu\text{m}$  features and appears to be a good fit with several of the features in the 7–12  $\mu\text{m}$  region. We calculated an integrated absorbance value for the 1084–1040 doublet of ethylene glycol at 300 K to be  $6.7 \times 10^{-18}$  cm molecule<sup>-1</sup>. Assuming that the 12  $\mu\text{m}$  signature is entirely due to synthesized ethylene glycol, we estimate that the percent of original CH<sub>3</sub>OH in the irradiated H<sub>2</sub>O+CH<sub>3</sub>OH ice converted to ethylene glycol is  $\sim 10\%$ . Spectrum (d) is the room temperature RESIDUE of a similarly irradiated H<sub>2</sub>O+CH<sub>3</sub>OH ice measured in our laboratory. The 1600 cm<sup>-1</sup> (6.3  $\mu\text{m}$ ) feature is attributed to C=O st mode of possibly carboxylic acid groups, the 1420 cm<sup>-1</sup> (7  $\mu\text{m}$ ) to C–H vibrations, and the 1050 cm<sup>-1</sup> (9.5  $\mu\text{m}$ ) to single bonded C–O vibrations. The RESIDUE was observed to slowly vaporize from an aluminum mirror over a period of days.

After irradiating these ices to different doses, spectra are analyzed to determine the molecular column density of synthesized species. We use the integrated absorbance values of  $2 \times 10^{-16}$  cm molecule<sup>-1</sup> for the 2340 cm<sup>-1</sup> C=O st of CO<sub>2</sub>,  $1.7 \times 10^{-17}$  cm molecule<sup>-1</sup> for the 2137 cm<sup>-1</sup> st of CO, and  $6 \times 10^{-18}$  cm molecule<sup>-1</sup> for the 1300 cm<sup>-1</sup> C–H deformation of CH<sub>4</sub> (values from Allamandola *et al.* (1988) and Sandford *et al.* (1988)). The CO/CO<sub>2</sub> and CH<sub>4</sub>/CO ratios are plotted in Fig. 5a and b, respectively, as a function of energy deposited per molecule in the ice. The eV molecule<sup>-1</sup> is calculated by using the linear energy transfer (LET) of 1 MeV protons, the total dose (protons cm<sup>-2</sup>), and the molecular density of the ice assuming a physical density of 1.0 g cm<sup>-3</sup> for H<sub>2</sub>O, CH<sub>3</sub>OH, and H<sub>2</sub>O ice mixtures.<sup>1</sup>

Figure 5a shows the calculated CO/CO<sub>2</sub> ratio for pure CH<sub>3</sub>OH and H<sub>2</sub>O+CH<sub>3</sub>OH as a function of eV molecule<sup>-1</sup>. Figure 5b is the CH<sub>4</sub>/CO ratio for the same experiments. The CO/CO<sub>2</sub> ratio decreases with increasing dose and approaches a value near 1.5 for the H<sub>2</sub>O > CH<sub>3</sub>OH mixture which is most relevant for astronomical applications. Several data points for similar mixtures irradiated with He ions from Baratta *et al.* (1994) begin at deposited energies above 20 eV molecule<sup>-1</sup> and indicate a ratio near 0.5. An explanation for the difference in their CO/CO<sub>2</sub> ratios may be that they perform a simultaneous deposition and irradiation since the penetration depth of the ions is of the order of 100 Å. Synthesized CO (and also CH<sub>4</sub> which is similar in volatility to CO) may be depleted from the ice surface before it is covered. Our results show that the CH<sub>4</sub>/CO ratio also decreases with increased proton dose and approaches a value near 2;

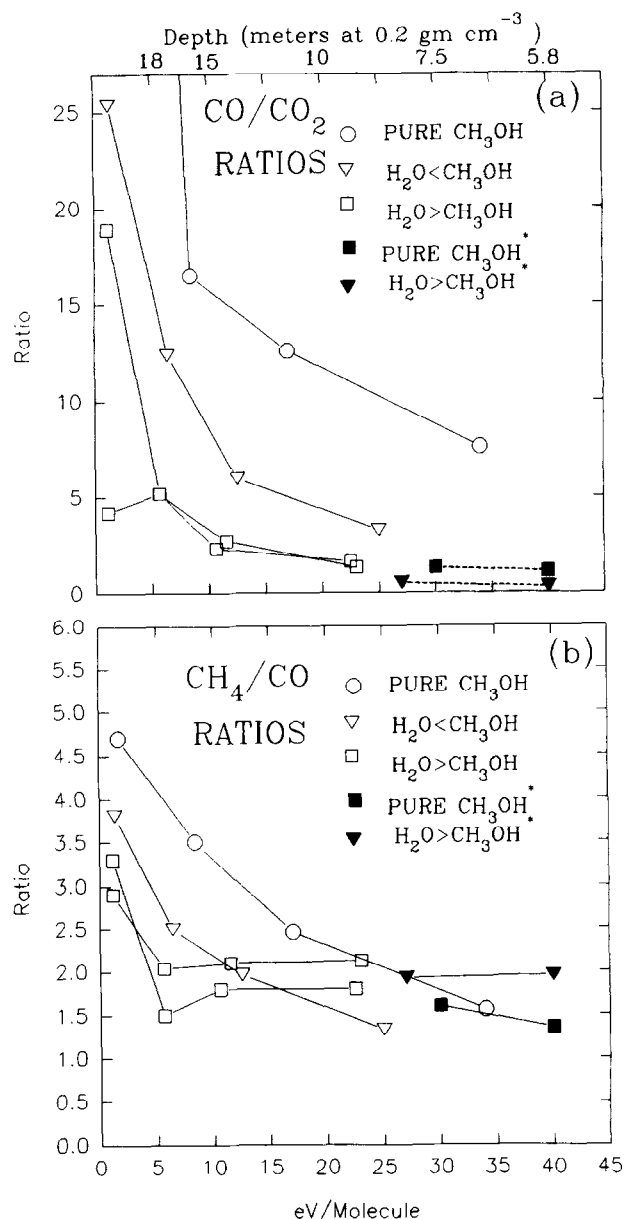


**Fig. 5.** Plots of the (a) CO/CO<sub>2</sub> and (b) CH<sub>4</sub>/CO ratios as a function of proton dose (eV molecule<sup>-1</sup>) for both pure CH<sub>3</sub>OH and H<sub>2</sub>O+CH<sub>3</sub>OH ices are shown. Data from He ion irradiation (\*Baratta *et al.*, 1994) are also included for comparison. The energy accumulated per molecule is related to the estimated dose accumulated by cometary ices due to cosmic ray bombardment during a 4.6 billion year storage time in the Oort cloud region (Strazzulla and Johnson, 1991). The top x-axis gives the estimate for the depth within a comet nucleus where similarly accumulated doses of energy are reached. The assumed density is 0.2 g cm<sup>-3</sup>. For cometary ices with a density of 1 g cm<sup>-3</sup>, multiply by 5

<sup>1</sup>The measured LET for 1 MeV protons in H<sub>2</sub>O is 308 MeV cm<sup>2</sup> g<sup>-1</sup> (Northcliffe and Shilling, 1970). Using the LET for H<sub>2</sub>O, we calculate a LET value of 320 MeV cm<sup>2</sup> g<sup>-1</sup> for CH<sub>3</sub>OH using a ratioing technique based on the stopping power equation (e.g. Swallow, 1973). The LET(MIXTURE) for H<sub>2</sub>O+CH<sub>3</sub>OH is LET(water)+LET(methanol) weighted by the percent abundance of each molecule. The eV molecule<sup>-1</sup> (MIXTURE) is calculated using LET(MIXTURE) and the molecular density (MIXTURE) which is also weighted by the percent abundance of each molecule in the mixture.

Baratta *et al.* (1994) give values near 2. We have calculated values for similar ratios from the results of Allamandola *et al.* (1988) on photolysed H<sub>2</sub>O+CH<sub>3</sub>OH (2:1) ices: CO/CO<sub>2</sub> = 4.3, and CH<sub>4</sub>/CO = 1 after 45 min of photolysis. It is not known what the equivalent eV molecule<sup>-1</sup> is for these experiments therefore we are not certain if these ratios represent the same amount of processing as our ices. Since the ratios are consistent with enhanced CO relative to the ratios in Fig. 5, one explanation could be

**Table 2.** Summary of ratios in  $p^+$  irradiated  $H_2O + CH_3OH$  (1:0.6) ice after an accumulation of  $22 \text{ eV molecule}^{-1}$ 

$CH_3OH/H_2O = 0.17$	$CH_3OH/H_2CO = 4.5$
$H_2CO/H_2O = 0.038$	
$CH_4/H_2O = 0.022$	$CH_4/CO = 1.96$
$CO/H_2O = 0.011$	
$CO_2/H_2O = 0.008$	$CO/CO_2 = 1.45$

that to a first approximation, once formed, CO is not readily photodissociated. In Fig. 5, the ratios at lower doses give valuable information that relates to possible product ratios deeper within the nucleus of a comet, as indicated by the top scale. Predicted values for the energy deposited in a comet over  $4.5 \times 10^9$  years are given by Moore *et al.* (1983) and references therein, and by Johnson (1991). In general at lower doses,  $CH_4 < CO$  and  $CO > CO_2$ .

For these experiments, the average initial ratio of  $CH_3OH/H_2O$  was 0.64 showing a typical ice spectrum in Fig. 2, and yielding typically the behavior plotted in Fig. 5a and b. The  $CH_3OH/H_2O$  ratio decreases with increasing irradiation and the synthesis of new carbon containing species. This ratio is determined using the area of the  $1021 \text{ cm}^{-1}$  line of  $CH_3OH$ , and the area of the  $1657 \text{ cm}^{-1}$  band of  $H_2O$ . Changes in this ratio are calculated assuming that the  $1021 \text{ cm}^{-1}$  feature is only due to  $CH_3OH$  (excluding contributions from any ethanol or acetone), and assuming that the area of the  $1657 \text{ cm}^{-1}$  band is unchanged with irradiation. We calculate a final ratio of  $CH_3OH/H_2O = 0.17$  after  $22 \text{ eV molecule}^{-1}$ , a decrease by a factor of 3.8. A similar analysis for the  $H_2CO/H_2O$  ratio is possible by curve fitting the  $1713 \text{ cm}^{-1}$  band and assuming that 25% of its area is due to  $H_2CO$ . We estimate in this way that a final ratio of  $H_2CO/H_2O \sim 0.038$  after  $22 \text{ eV molecule}^{-1}$ . Table 2 summarizes the calculated ratios of these and other products.

A study of the number of synthesized molecules formed in irradiated thin ice films deposited on aluminum mirror substrates, compared with similar ices supported on silicate smoke layers, is currently in progress. In this paper we report on the spectra of  $CH_3OH$  ice deposited at  $T < 20 \text{ K}$  on silicate smoke layers. Instead of forming a completely amorphous phase spectrum, it appears mostly crystalline (Moore *et al.*, 1994). Spectra of  $CH_3OH$  on silicate before and after irradiation is shown in Fig. 6. A comparison of spectrum (a) with the analogous spectrum (a) from Fig. 1 shows the sharpness of several  $CH_3OH$  features along with some splitting associated with the more crystalline phase of  $CH_3OH$  on the silicate smoke. Spectra shown in Fig. 6 have been ratioed with the blank silicate smoke

spectrum taken before any gas condensation. This process removes the large  $10 \mu\text{m}$  silicate feature and reveals the structure of the deposited ice in that region. After irradiation, new species have been identified. A comparison of trace (b) in Figs 1 and 6 shows that there are similarities between the products. Some CO is synthesized, but its IR absorption feature is measurable only after scale expansion. Relative to the results shown in Fig. 1 for irradiated  $CH_3OH$  on aluminum substrates, for irradiated  $CH_3OH$  on silicate smoke we detect less CO and  $H_2CO$  than  $CH_4$ . A major change between spectrum (a) and spectrum (b) is the radiation-induced amorphization (phase change) of the  $CH_3OH$ . Like irradiated  $CH_3OH$  on aluminum, irradiated  $CH_3OH$  ice on silicate smoke does not convert to a crystalline phase with warming. A quantitative analysis for these results, which incorporated a meaningful analysis of the LET and  $\text{eV molecule}^{-1}$  calculations for an ice/silicate composite is underway. Problems can arise with the ratioing technique after irradiation causing some irregularities in the baseline near the edges of the wavelength region marked with the line in Fig. 6. Possibly the thickness of the silicate smoke changes and/or defect formation within the silicate occurs affecting the  $10 \mu\text{m}$  feature. However, most regions of the spectrum are undisturbed.

## Discussion

$H_2CO$  is the dominant volatile species identified in irradiated  $H_2O + CH_3OH$  using IR spectra. This is consistent with the photolysis results reported by Allamandola *et al.* (1988). Other volatile species which are easily identified are, in order of abundance,  $CH_4$ , CO, and  $CO_2$ . Ethylene glycol is identified with several IR features in the irradiated mixture after warming to  $T \sim 200 \text{ K}$ . The identification of the molecular composition of the residue will require further investigations using GC-MS analysis. The IR spectrum of the residue is consistent with the identification of some combination of polyalcohols and glycols, and with carboxyl group molecules. It is representative of one type of organic material which could exist in the outer layers of comets and contribute to the variety of organic grains detected during the Halley flyby (see review by Fomenkova *et al.* (1994) and references therein).

The data set consisting of ion irradiation (this study and Baratta *et al.* (1991)) and UV photolysis results (Allamandola *et al.*, 1988) on  $H_2O + CH_3OH$  ice is one example of only a few existing sets of data which can be compared. In the  $H_2O + CH_3OH$  case, all of the IR results are remarkably similar at  $T < 20 \text{ K}$ . However, there are fundamental differences between photochemical mechanisms produced by UV photons and radiation-chemical mechanisms due to protons, and it is important to carry out both types of experiments.<sup>2</sup>

Our results show a gradual decrease in the  $CH_3OH/H_2O$  ratio with increased irradiation. The binary mixture used in the laboratory is a gross simplification for the complex icy mixture expected in comets. However, we can apply the trends to show what we would expect for  $CH_3OH$  in

<sup>2</sup>Only light absorbed by a molecule can be effective in producing a photochemical change, and the light is absorbed in a quantum process. Typical photons initiate reactions with a single molecule within a few hundred ångströms of the surface. Protons lose energy in discrete processes to electrons in the stopping medium and undergo a large number of interactions. The range of a 1 MeV proton is  $10^{-2}$ – $10^{-3} \text{ cm}$  in typical organic material with densities near  $1 \text{ g cm}^{-3}$ . More energetic ions penetrate to greater depths.

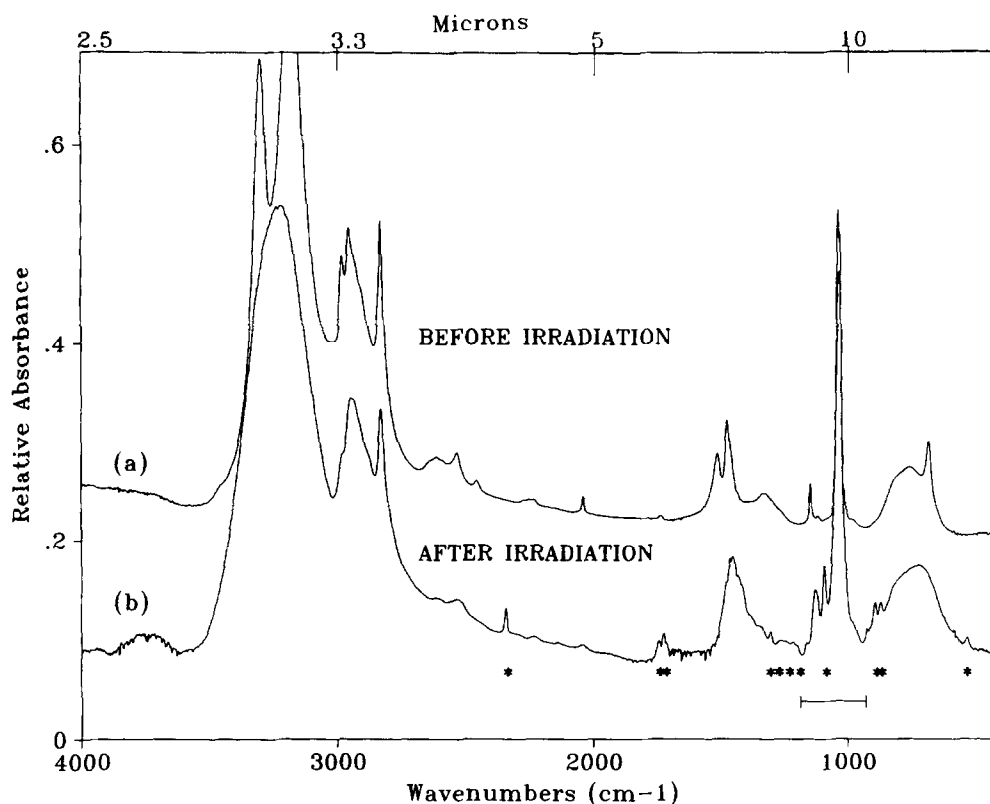


**Fig. 6.** (a) Infrared spectrum of  $\text{CH}_3\text{OH}$  ice formed on a silicate smoke layer at  $T < 20$  K. (b) The same ice after proton irradiation. Before irradiation the ice is mostly crystalline in phase. Irradiation amorphization occurs during bombardment. Most synthesized species marked with an asterisk are identified in Table 1. The  $10 \mu\text{m}$  silicate feature has been removed by ratioing each trace with the spectrum of the silicate smoke before any ice condensed. Ratioing may cause some irregularity in the baseline in the wavelength region marked with a line

comets. A comet originally containing a similar  $\text{H}_2\text{O}$  and  $\text{CH}_3\text{OH}$  ice component would have a decreasing concentration of  $\text{CH}_3\text{OH}$  toward its outer layers due to cosmic ray processing during storage in the Oort cloud (if independent of all other sources and sinks). When dynamically new, the release of volatiles from the most heavily irradiated outer layers of ices could give  $\text{CH}_3\text{OH}/\text{H}_2\text{O}$  ratios a factor of at least 4 lower than the deep ices which are most pristine and minimally processed. Dynamically new comets would have  $\text{CO} > \text{CO}_2$  by a factor of  $\sim 1.5$ . As these comets age, in the absence of additional processing, you would expect to see a continuous increase in the  $\text{CH}_3\text{OH}$  abundance and a decrease in  $\text{H}_2\text{CO}$ ,  $\text{CH}_4$ ,  $\text{CO}$ , and  $\text{CO}_2$  as less irradiated ices are exposed.

The  $\text{CH}_3\text{OH}$  abundance has been tabulated for several recent comets (Eberhardt *et al.*, 1994). There exists clear variations between comets; abundances from values near a few tenths of a percent to 7% (relative to  $\text{H}_2\text{O}$ ) have been reported. In general these values are compatible with the range of values observed in interstellar environments. Mumma *et al.* (1993b) have argued that, based on the  $\text{CH}_3\text{OH}$  abundance, comets tend to fall into two groups. Those comets with higher  $\text{CH}_3\text{OH}$  abundances tend to be dynamically new, and those with lower abundances tend to be short-period. Mumma *et al.* (1993b) suggest that a cosmogenic connection could account for the compositional dichotomy. These  $\text{CH}_3\text{OH}$  abundances are

opposite to what we would expect based on our laboratory experiments *if* short-period comets are assumed to be evolved older comets, but this assumption is a simplification of a complex problem. Comets might form in different regions with different  $\text{CH}_3\text{OH}$  enrichments, or comets might form in the same region but at different times when the precomet material contains different  $\text{CH}_3\text{OH}$  enrichments. For example, late forming comets could contain less  $\text{CH}_3\text{OH}$  if the precomet material has undergone increased irradiation due to a decrease in the opacity of the nebula. Additional comet observations are necessary to improve the statistics of the  $\text{CH}_3\text{OH}$  abundance–dynamic age correlation as pointed out by Eberhardt *et al.* (1994).

Infrared spectra of  $\text{CH}_3\text{OH}$  at  $T < 20$  K on silicate smokes reveal that predominantly crystalline phase ice forms directly on deposit. A mechanism to explain this is currently under investigation. In a separate experiment with silicate smokes, we have found that condensed  $\text{H}_2\text{CO}$  in a mixture with  $\text{H}_2\text{O}$  is not retained during warming to as high a temperature as similar deposits (which form as amorphous phase deposits) on aluminum substrates (Ferrante *et al.*, 1994). We have not completed the study of the residues formed from these irradiated ice/silicate composites. More realistic cometary type mixtures may be quite complex. For example, from past experiments we know that noble gases are more effectively trapped in irradiated silicates than in unirradiated silicates (Nichols



*et al.*, 1992). The idea that irradiation produces active sites in silicates which are in intimate association with icy mixtures suggests that in these more complex mixtures, volatile material may compete for trapping sites after irradiation. The idea that amorphous ices retain volatile species is central to many cometary theories. Since the laboratory produced silicates have such a dramatic effect on the phase of the ice, and radiation may change trapping sites within the silicate, we are studying ices/silicate composites and their radiation products in an effort to understand the ice/surface interactions which affect the retention of volatiles.

*Acknowledgements.* The authors thank Reggie Hudson for math transforms, and Steve Brown and members of the GSFC/Radiation Facility for the operation of the accelerator. We acknowledge NASA funding support through Grant NSG 5172.

## References

- Allamandola, L. J., Sandford, S. A. and Valero, G. J., Photochemical and thermal evolution of interstellar/precometary ice analogs. *Icarus* **76**, 225–252, 1988.
- Baratta, G. A., Leto, G., Spinella, F., Strazzulla, G. and Foti, G., The 3.1  $\mu\text{m}$  feature in ion-irradiated water ice. *Astron. Astrophys.* **252**, 421–424, 1991.
- Baratta, G. A., Castorina, A. C., Leto, G., Palumbo, M. E., Spinella, F. and Strazzulla, G., Ion irradiation experiments relevant to the physics of comets. *Planet. Space Sci.* **42**, 759–766, 1994.
- Baxendale, J. H. and Mellows, F. W., The  $\gamma$ -radiolysis of methanol and methanol solutions. *J. Am. Chem. Soc.* **83**, 4720–4726, 1961.
- Combes, M. *et al.*, The 2.5–12  $\mu$  spectrum of Comet Halley from the IKS-Vega experiment. *Icarus* **76**, 404–436, 1988.
- Eberhardt, P., Meier, R., Krankowsky, D. and Hodges, R. R., Methanol and hydrogen sulfide in comet P/Halley. *Astron. Astrophys.* **288**, 315–329, 1994.
- Ferrante, R. F., Moore, M. H. and Nuth III, J. A., Laboratory studies of formaldehyde polymerization in cometary ice analogues. *BAAS* **26**(3), 1121, 1994.
- Fomenkova, M. N., Chang, S. and Mukhin, L. M., Carbonaceous components in the comet Halley dust. *Geochim. Cosmochim. Acta* **58**, 4503–4511, 1994.
- Greenberg, J. M., Physical, chemical and optical interactions with interstellar dust, in *Chemistry in Space* (edited by J. M. Greenberg and V. Pirronello), pp. 227–271. Kluwer, The Netherlands, 1991.
- Grim, R. J. A., Baas, F., Geballe, T. R., Greenberg, J. M. and Schutte, W., Detection of solid methanol toward W33A. *Astron. Astrophys.* **243**, 473–477, 1991.
- Hagen, W., Tielens, A. G. G. M. and Greenberg, J. M., A laboratory study of the infrared spectra of interstellar ices. *Astron. Astrophys. Suppl. Ser.* **53**, 389–416, 1983.
- Hobbs, D. V., in *Ice Physics*, 1st edn, pp. 44–60. Clarendon Press, Oxford, 1974.
- Hudson, R. L. and Moore, M. H., Far-IR spectral changes accompanying proton irradiation of solids of astrochemical interest. *Radiat. Phys. Chem.* **45**(5), 779–789, 1995.
- Johnson, R. E., Irradiation effects in a comet's outer layers. *J. Geophys. Res.* **96**(E2), 17,553–17,557, 1991.
- Kalyazin, E. P. and Kovalev, G. V., Effect of temperature on the radiolysis of methanol. *High Energy Chemistry* **12**, 313–314, 1978.
- Kouchi, A., Yamamoto, T., Kozasa, T., Kuroda, R. and Greenberg, J. M., Conditions for condensation and preservation of amorphous ice and crystallinity of astrophysical ices. *Astron. Astrophys.* **290**, 1009–1018, 1994.
- Moore, M. H. and Hudson, R. L., Far-infrared spectral studies of phase changes in water ice induced by proton irradiation. *Astrophys. J.* **401**, 353–360, 1992.
- Moore, M. H. and Hudson, R. L., Far-infrared spectra of cosmic-type pure and mixed ices. *Astron. Astrophys. Suppl. Ser.* **103**, 45–56, 1994.
- Moore, M. H. and Khanna, R., Studies of proton irradiated  $\text{H}_2\text{O} + \text{CO}_2$  and  $\text{H}_2\text{O} + \text{CO}$  ices and analysis of synthesized molecules. *J. Geophys. Res.* **96**(E2), 17,541–17,545, 1991.
- Moore, M. H., Donn, B., Khanna, R. and A'Hearn, M. F., Studies of proton irradiated cometary-type ice mixtures. *Icarus* **74**, 388–405, 1983.
- Moore, M. H., Ferrante, R. F., Hudson, R. L. and Nuth III, J. A., Infrared spectra of crystalline phase ices condensed on silicate smokes at  $T < 20$  K. *Astrophys. J.* **428**, L81–L84, 1994.
- Mumma, M. J., Weaver, H. A., Larson, H. P. and Davis, D. S., Detection of water vapor in Halley's Comet. *Science* **232**, 1523–1528, 1986.
- Mumma, M. J., Weissman, P. R. and Stern, S. A., Comets and the origin of the solar system: reading the Rosetta Stone, in *Protostars and Planets III* (edited by E. H. Levy, J. I. Lunine and M. A. Matthews), pp. 1177–1252. Univ. of Arizona Press, Tucson, 1993a.
- Mumma, M. J., Hoban, S., Reuter, D. C. and DiSanti, M., Methanol in recent comets: evidence for two distinct populations. *BAAS* **25**(3), 1065, 1993b.
- Nichols Jr, R. H., Nuth III, J. A., Hohenber, C. M. and Olinger, C. T., Trapping of noble gases in proton-irradiated silicate smokes. *Meteoritics* **27**, 555–559, 1992.
- Northcliffe, L. C. and Shilling, R. F., Range and stopping power tables for heavy ions. *Nucl. Data Tables A7*, 233–463, 1970.
- Omont, A., Moseley, S. H., Forveille, T., Giaccum, W. J., Harvey, P. M., Likkel, L., Loewenstein, R. F. and Lisse, C. M., Observations of 40–70 micron bands of ice in IRAS 09371 + 1212 and other stars. *Astrophys. J.* **355**, L27–L30, 1990.
- Porter, R. P. and Noyes Jr, W. A., Photochemical studies. LIV. Methanol vapor. *J. Am. Chem. Soc.* **81**, 2307–2311, 1959.
- Sandford, S. A., Allamandola, L. J., Tielens, A. G. G. M. and Valero, G. J., Laboratory studies of the infrared spectral properties of CO in astrophysical ices. *Astrophys. J.* **329**, 498–510, 1988.
- Skinner, C. J., Tielens, A. G. G. M., Barlow, M. J. and Justtanont, K., Methanol ice in the protostar GL 2136. *Astrophys. J.* **399**, L79–L82, 1992.
- Spinrad, J., Comets and their composition. *Ann. Rev. Astron. Astrophys.* **25**, 231–269, 1987.
- Strazzulla, G. and Johnson, R. E., Irradiation effects on comets and cometary debris, in *Comets in the Post-Halley Era* (edited by R. L. Newburn Jr *et al.*), pp. 243–275. Kluwer, The Netherlands, 1991.
- Strazzulla, G., Leto, G., Baratta, G. A. and Spinella, F., Ion irradiation experiments relevant to cometary physics. *J. Geophys. Res.* **96**, 17,547–17,552, 1991.
- Swallow, A. J., *Radiation Chemistry—An Introduction*, p. 31. Wiley, New York, 1973.
- Tielens, A. G. G. M., Dust in dense clouds, in *Interstellar Dust* (edited by L. J. Allamandola and A. G. G. M. Tielens), pp. 239–262. IAU, 1989.